GEOPHYSICAL RESEARCH LETTERS, VOL. 25, NO.11, PAGES 1899-1902, JUNE 1, 1998

Effects of cloud shape and water vapor distribution on solar absorption in the near infrared

Igor A. Podgorny, Andrew M. Vogelmann, and V. Ramanathan

Center for Atmospheric Sciences, Scripps Institution of Oceanography, La Jolla, California

Abstract. A 3D Monte Carlo radiative transfer model is used to demonstrate the importance of cloud shape and water vapor distribution on narrow-band solar absorption at 0.93 and 2.0 μm. Diurnally averaged absorption for wavy-topped broken cloud fields can exceed that based on conventional climate model assumptions (plane-parallel cloud geometry and an unsaturated water vapor distribution in gaps between cloud elements) by 2-10% of the top-of-atmosphere insolation. Plane-parallel clouds often underestimate the absorption by non-flat-top clouds, particularly at 2.0 μm and large solar zenith angles. Ambiguities in assigning the above-cloud water vapor profile create uncertainties in the absorption comparisons between the plane-parallel and non-flat-top clouds, which increase with solar zenith angle and may be as large as 5 to 8%. A thin saturated water vapor layer (0.4 km) above the cloud top systematically enhances column absorption, the magnitude depends on cloud altitude and wavelength. Thus, realistic 3-D distributions of cloud shape, brokenness and water vapor are needed to quantify the role of clouds in excess absorption.

Introduction

Recent studies and debates have focused on excess absorption, defined as an unexplained, systematic and significant positive difference between observed and modeled atmospheric absorption (for reviews, see Stephens and Tsay [1990] and Ramanathan and Vogelmann [1997]). Globally and diurnally averaged, the model absorption is suggested to be smaller than that observed by about 6 to 8 % of the insolation at the top-of-the atmosphere (TOA), or about 20 to 25 W m^{-2} [e.g. Arking 1996 and Wild et al. 1995], but these numbers are being challenged [e.g. Francis et al. 1997]. The objective of this paper is to explore the potential biases in models due to two major approximations invoked in most climate models: plane-parallel (PP) clouds and identical water vapor distributions in clear and overcast skies.

The cloud radiative effect is observationally determined from satellite, surface or aircraft measurements as the difference between the cloudy sky flux and the clear sky flux. (Clear sky here means there are no clouds in the atmospheric column. Cloudy sky means that clouds exist in the atmospheric column, but it need not be overcast.) The cloud layer observed is generally saturated with respect to water vapor while the corresponding level is not saturated in the clear sky case. However, in climate model radiative transfer calculations, the water vapor profile typically is a single sample or regional average, which does not recognize the true 3D water vapor variability and it is even possible that the modeled cloud layer is not saturated. Further, Crisp [1997] suggests that "an additional absorber that is concentrated above the cloud tops is needed to produce a cloud shortwave forcing that is more independent of solar zenith angle, like that observed" and suggests that aerosols might provide this opacity. However, a saturated layer of water vapor above the cloud could have a similar effect, and the existence of such a layer is not inconsistent with some observations showing that a substantial amount of saturated or near-saturated water vapor can exist above or around some clouds [Radke and Hobbs 1991; Smith 1992; Perry and Hobbs 1994]. Thus, we determine the potential effects on solar absorption of such features in the water vapor profiles that are normally ignored.

Also, theoretical evidence indicates that absorption of solar radiation in a cloudy atmosphere is a complex function of the cloud shape. It may be sensitive to cloud geometry for tropical cumulus clouds [e.g., O'Hirok and Gautier 1997] or nearly insensitive to the cloud shape for quasi-stratiform fractal clouds [e.g., Marshak et al. 1997].

In this paper, we couple a Monte Carlo (MC) code to a correlated k-distribution model to study absorption in 3D cloudy atmospheres. We consider: (1) wavy cloud tops to highlight the limitations of the flat cloud top models in climate calculations; (2) broken clouds to examine the biases of PP clouds for partially cloudy scenes; and (3) unsaturated and saturated (in cloudy layers) water vapor distribution with particular emphasis on the layer immediately above the cloud tops. We limit ourselves to the case of quasi-stratiform clouds, a major component of the global cloud cover.

Radiative Transfer Model

The MC model follows an algorithm by Marchuk et al. [1980] in sampling the photon trajectories and directions of the photon's motion. Generalization of the algorithm for the case of 3D clouds is done based on the Maximum Cross-Section Method [Marchuk et al. 1980]. We assume that the water vapor distribution is PP and that the water drop optical properties are homogeneous within the clouds. A Henyey-Greenstein phase function is used. We consider an aerosol-free atmosphere, non-reflecting surface and neglect absorption by gases other than water vapor. Atmospheric water vapor transmission is computed using correlated k-distributions and applied as a correction to the photon's weight. We use 20 k-coefficients per band which provides an accuracy better than 1%, which is consistent with the typical statistical error of MC methods, usually being between 0.1 and 1%.

We select the 0.93-0.94 μm band (hereafter referred to as 0.93 μm band) to represent an upper limit for water vapor absorption. The band is located in the center of a strongly absorbing water vapor band, and the cloud drop single-scattering albedo (ϖ) is close to 1 so that cloud drop absorp-

Paper number 98GL01444.
0094-8534/98/98GL-01444$05.00

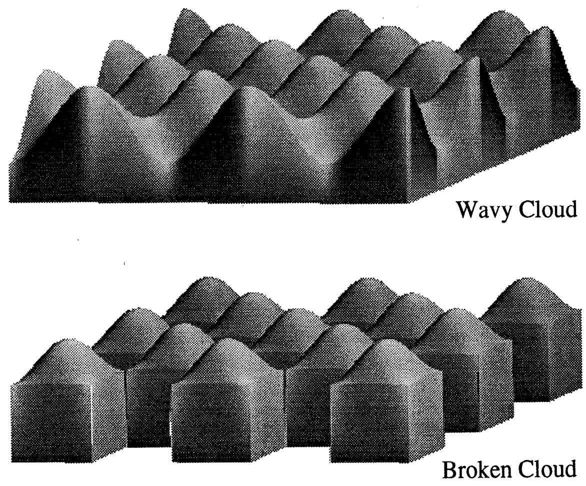

Figure 1. The cloud configurations. Wavy clouds: mean optical thickness - 15, mean geometrical thickness - 0.4 km, wave amplitude - 0.2 km, wavelength - 1 km. Broken clouds: mean optical thickness - 7.5, horizontal length of cloud gaps - 0.5 km, cloud fraction - 50%.

tion is negligible. We use ϖ=0.9999 and an asymmetry parameter g=0.84 computed with a Mie code for a stratus cloud size distribution with an effective droplet radius of 5 μm. We next consider the other extreme: the 2.00-2.01 μm band (hereafter referred to as 2.0 μm band), in which water drop absorption is strong (ϖ=0.97, g=0.79), and the water vapor absorption is weak. We neglect absorption by CO_2 in 2.0 μm band to accentuate the effect of water vapor absorption.

We use two cloud base altitudes, 1 km (low level cloud) and 5 km (mid-level cloud). The first cloud configuration treated in the model is a conventional PP cloud. The second one, "wavy cloud", has the same cloud base as the PP cloud, but the top surface is a 2D sinusoidal wave with wavelengths of 1 km in x and y directions. The mean geometrical thickness of the cloud and the wave amplitude are 0.4 and 0.2 km, respectively. The third cloud configuration, "broken cloud", is created from the second one by putting the holes in the cloud when the sinusoid is negative so that the cloud fraction is 50% (see Figure 1). We compare absorption by the broken cloud field to that in an atmosphere consisting of two equal parts of clear skies and either the wavy or PP clouds; the latter case is that used in climate models. The mean optical thickness is 15 for PP and wavy clouds, and 7.5 for broken clouds; thus, the mean optical thickness and cloud fraction of the hybrid systems are equal to those for the broken cloud layer. No altitude-dependent changes are made to the cloud properties.

The PP saturated water vapor layer extends from cloud base to the maximum height of the sinusoidal cloud top, has a thickness of 0.6 km and is referred to hereafter as the standard water vapor distribution. We also use an "extended" water vapor distribution produced by placing an additional 0.4 km of saturated water vapor over the cloud top, which is consistent with some observations of saturated or near-saturated water vapor above the clouds [e.g. Smith 1992]. Water vapor concentrations above cloud top and below cloud base are obtained from a typical clear sky October day from the Oklahoma ARM site during ARESE-1995 experiment. Vertical resolution for all profiles is 0.2 km. The column water amount is 1.40 cm (clear sky), 1.76 and 1.53 cm (standard distributions, 1 and 5 km, respectively), 1.87 and 1.57 cm (extended distributions, 1 and 5 km, respectively).

To bracket the ambiguity associated with comparing PP and 3D clouds with wavy tops, two PP cloud top heights are used. First, the mean PP geometrical thickness is 0.2 km so its upper bound corresponds to the bottom of the wave of the wavy cloud. Second, the geometrical thickness is 0.6 km, matching the thickness of the saturated water vapor layer and the upper bound of the wavy cloud top. The PP extinction coefficient is adjusted to hold the optical depth constant at 15 for the different cloud thicknesses.

Results of Calculations and Conclusions

The results are expressed in terms of fractional column absorption of the incident TOA flux calculated for solar zenith angles ranging from 0 to 80°; the column extends from the surface to the TOA. For clear, unsaturated skies, fractional absorption increases with solar zenith angle from 55 to 85% in 0.93 μm band, and from 15 to 40% in 2.0 μm band. When the 1.0-1.6 km layer is saturated, the fractional absorption increases (absolute increase) by 5% and 4.5% in the 0.93 μm and 2.0 μm bands, respectively. Effects of saturation in the 5.0-5.6 km layer are relatively small for these bands (1.5% and 1% respectively).

Figures 2-3 show the fractional absorption for broken clouds for the standard water vapor distribution, and for the 50% clear sky hybrids with the 50% wavy or PP clouds. Note

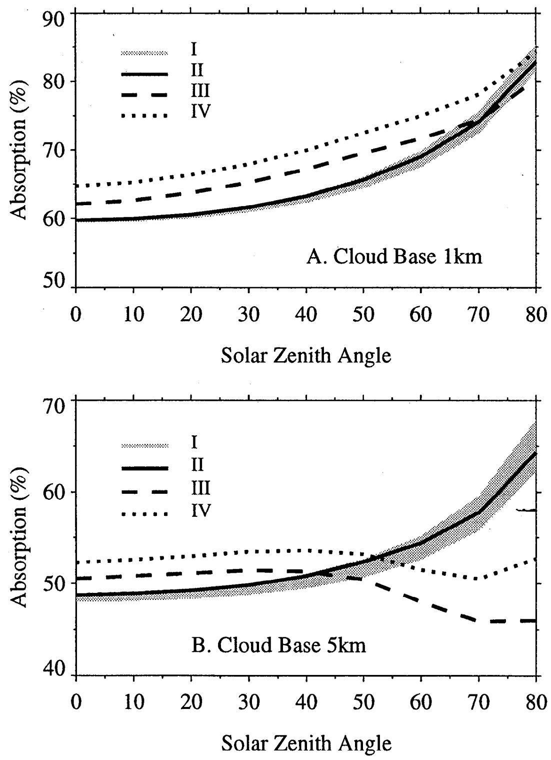

Figure 2. Fractional absorption in the 0.93 μm band for 50% cloud coverage. Calculations are made for standard (0.6 km) saturated water vapor profile (I - PP, II - wavy clouds and III - broken clouds), and extended (1 km) saturated water vapor profile (IV - broken clouds). The wavy and PP cloud hybrids are unsaturated in the cloud gaps. The upper bound of the shaded region is for a PP cloud with a thickness of 0.2 km; the lower bound is for a 0.6 km thick PP cloud.

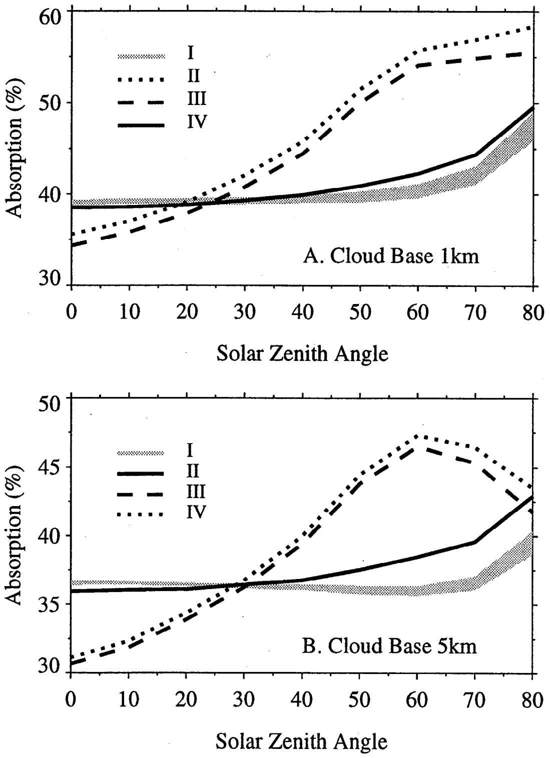

Figure 3. As in Figure 2 but for 2.0 μm band.

that the cloud gaps are unsaturated in the hybrid wavy and PP cloud fields, but are saturated in the broken cloud layer. The use of shading instead of a line for PP clouds is a consequence of the uncertainty in choosing the cloud top height (two different cloud top heights are applied to the same water vapor profile). Diurnal averages of the results shown in Figures 2 and 3 are presented in Table 1, which also includes results for unsaturated profiles. Diurnal averages for clear sky case are 65.9% for 0.93 μm band and 22.4% for 2.0 μm band.

The common features in Figures 2 and 3 follow. A) PP clouds often underestimate the narrow-band absorption by the 3D, non-flat-top clouds at 2.0 μm, where differences between cloud shapes are most pronounced here. PP clouds underestimate the diurnally averaged, fractional absorption by 2 to 10%, and the differences are as large as 10 to 15% at specific solar zenith angles. B) Ambiguities in assigning the above-cloud water vapor distribution results in a diurnally averaged difference in the PP results of 1 to 2%. The difference increases with solar zenith angle, water vapor absorption, and the range (given by shading) is as much as 5 to 8% at specific solar zenith angles. C) A 0.4 km thick, overlying saturated layer (extended water vapor layer) results in additional absorption for all cases, with increases of 2 to 6%, which depends on wavelength, cloud height and solar zenith angle. D) Low, broken clouds can enhance absorption by 2 to 10% (diurnal average) relative to the other clouds.

The solar zenith angle dependence of absorption by the broken clouds is different from the pattern shown by the PP and wavy clouds. At 0.93 μm, the low broken cloud absorption is enhanced for most sun angles because the region between the broken clouds is saturated (unlike the 50% subsaturated clear region). These results are qualitatively similar to those for the low cloud case by O'Hirok and Gautier [1997], but differences between our cloud geometries prevent a quantitative comparison. However, absorption for broken mid-level clouds decreases for slant solar zenith angles (Figure 2B) because the broken cloud field shades the water vapor below the clouds, where most of the water vapor resides. The absorption for the 0.93 μm PP and wavy cloud hybrids increases more quickly with sun angle than for the broken clouds because the associated water vapor absorption increase in the 50% clear-sky portion cannot be shaded by the clouds. The effect of brokenness on solar absorption reverses dramatically in the spectral region where cloud drops absorb (Figure 3B) because, at slant angles, the direct solar beam for the broken cloud field becomes filled by clouds, but the clear 50% portions in the hybrid cases are never filled.

We further quantify the effect of water vapor on absorption by repeating all cloud cases with an unsaturated clear sky water vapor profile (Table 1), thereby minimizing water vapor absorption. This reduces the 0.93 μm absorption for the low broken clouds so that there is nearly no cloud shape effect, which is in agreement with results reported by Marshak et al. [1997]. This indicates the importance of saturating the cloud layer in radiative transfer calculations. However at 2.0 μm, saturated and unsaturated cases are nearly equal.

Since the 0.93 μm and 2.0 μm bands represent two limiting cases with respect to water vapor and water drop absorption, the conclusions derived from the narrow-band calculations should bracket the range of additional solar absorption at other wavelengths. Also, broadband absorption should increase in the presence of a saturated water vapor layer overlying the cloud tops. We demonstrate this with PP, broadband calculations (from 0.5 to 3.5 μm) made with a discrete ordinate method algorithm [Stamnes et al. 1988]. The model uses four streams and include Rayleigh scattering, and water vapor absorption computed with correlated k-distributions. The correlated k-distributions and scattering properties of clouds are treated as before, but are computed for the 100 bands used to cover the 0.5 to 3.5 μm wavelength region.

We find that an overlying saturated layer of 0.4 km enhances cloud absorption (at 1 and 5 km), yielding a diurnal average enhancement at the ARM Oklahoma site for mid-October of approximately 1.1% for 100% cloud cover, and half that for 50% cloud cover. This is consistent with results

Table 1. Diurnal average fractional absorption (%) for the Oklahoma ARM site (mid-October) calculated for saturated and unsaturated (in parentheses) water vapor profiles. The range given for the PP cases gives the ambiguity in choosing the cloud top for comparison with the non-flat-top clouds. The diurnal averages apply only to the solar geometry specified by this latitude and time of year. Notation for cloud cases is the same as in Figures 2-3.

	0.93 μm		2.0 μm	
	1 km	5 km	1 km	5 km
I	67.0-69.1 (64.7-65.7)	52.4-54.9 (50.0-50.6)	40.0-41.4 (39.5-40.2)	36.0-36.7 (35.8-36.0)
II	68.3 (65.3)	54.1 (50.7)	42.1 (41.3)	38.3 (37.8)
III	71.1 (65.5)	49.1 (43.9)	51.3 (49.1)	43.9 (42.9)
IV	74.2	52.5	52.9	44.7

by Davies et al. [1984] who demonstrated the importance to absorption of above-cloud unsaturated water vapor.

One conclusion of this paper is that an important uncertainty in comparing the absorption computed for PP clouds to those with complicated cloud tops is the treatment of the saturated water distribution within and around the cloud. The question of applicability of a quasi-3D approach (1D, plane-parallel water vapor distribution plus 3D clouds as we have assumed here) to modeling radiative transfer in a cloudy atmosphere is open and remains beyond the scope of this study.

At the moment we note that the area surrounding the real clouds exhibits plenty of 3D variability in water vapor content [e.g., Radke and Hobbs 1991; Perry and Hobbs 1994], but we cannot present quantitative information on how water vapor and liquid water are distributed relative to each other. Although considerable progress has been made in fractal models to challenge 3D liquid water distribution [e.g. Marshak et al. 1997], similar advances for the water vapor distribution are needed. More detailed observational efforts combined with applying 3D MC models for processing and understanding the data of solar energy absorption in a cloudy atmosphere are required to properly address the excess absorption question.

Acknowledgments. The authors thank W. Ridgway for providing the k-distribution code and A. Arking and an anonymous reviewer for valuable comments on the manuscript. This work was supported by DOE ARM grant DE-FG03-91ER61198 and by the NSF Science and technology Center for Clouds, Chemistry and Climate (C4), and is C4 publication 189.

References

Arking, A., Absorption of solar energy in the atmosphere: Discrepancy between model and observations, *Science, 273*, 779-782, 1996.

Crisp, D., Absorption of sunlight by water vapor in cloudy conditions: A partial explanation for the cloud absorption anomaly, *Geophys. Res. Lett., 24*, 571-574, 1997.

Davies, R., W.L. Ridgway, and K.-E. Kim, Spectral absorption of solar radiation in cloudy atmospheres: A 20 cm^{-2} model, *J. Atmos. Sci., 41*, 2126-2137, 1984.

Francis, P.N., J.P. Taylor, P. Hignett, and A. Slingo, On the question of enhanced absorption of solar radiation by clouds, *Q. J. R. Meteorol. Soc., 123*, 419-434, 1997.

Marchuk, G.I., G.A. Mikhailov, M.A. Nazaraliev, R.A. Darbinjan, B.A. Kargin, and B.S. Elepov, *The Monte Carlo methods in atmospheric optics*, Springer Searies in Optical Sciences, Springer, Berlin, 1980.

Marshak, A., A. Davis, W. Wiscombe, W. Ridgway, and R. Cahalan, Biases in shortwave column absorption in the presence of fractal clouds, *J. Clim., 11*, 431-446, 1998.

O'Hirok, W., and C. Gautier, Spectral aspects of three-dimensional atmospheric absorption, Preprints, *Ninth Conference on Atmospheric Radiation*, February 2-7, 1997, Long Beach, California, 19-21, 1997.

Perry, K.D., and P.V. Hobbs, Further evidence for particle nucleation in clear air adjacent to marine cumulus clouds, *J. Geophys. Res., 99*, 22,803-22,818, 1994.

Radke, L.E., and P.V. Hobbs, Humidity and particle fields around some small cumulus clouds, *J. Atmos. Sci., 48*, 1190-1195, 1991.

Ramanathan, V., and A.M. Vogelmann, Greenhouse effect, atmospheric solar absorption and the Earth's radiation budget: From the Arrhenius-Langley Era to the 1990s, *Ambio, 26*, 38-46, 1997.

Smith, R.B., Deuterium in North Atlantic storm tops, *J. Atmos. Sci., 49*, 2041-2057, 1992.

Stamnes, K., S.-C. Tsay, W. Wiscombe, and K. Jayaweera, Numerically stable algorithm for discrete-ordinate-method radiative transfer in multiple scattering and emitting layered media, *Appl. Opt., 27*, 2502-2509, 1988.

Stephens, G.L., and S.-C. Tsay, On the cloud absorption anomaly, *Q. J. R. Meteorol. Soc., 116*, 671-704, 1990.

Wild, M., A. Ohmura, H. Gilgen, and E. Roeckner, Validation of general circulation model radiative fluxes using surface observations, *J. Clim., 8*, 1309-1324, 1995.

I. Podgorny, A. Vogelmann, and V. Ramanathan, Center for Atmospheric Sciences, Scripps Institution of Oceanography, 9500 Gilman Drive, La Jolla, CA 92093-0221. (e-mail: igor@fiji.ucsd.edu)

(Received July 10, 1997; revised February 9, 1998; accepted April 17, 1998.)